

Research Article/Araştırma Makalesi

Mathematical modeling of a photovoltaic/thermal (PV/T) collector

Gamze Soytürk¹, Onder Kızıllkan¹, Mehmet Akif Ezan²

¹Isparta University of Applied Sciences, Faculty of Technology, Mechanical Engineering, 32200, Isparta, Turkey

²Dokuz Eylül University, Faculty of Engineering, Mechanical Engineering, 35040, İzmir, Turkey

Keywords

Photovoltaic/Thermal
collector
Solar energy
Thermal efficiency
Electrical efficiency

Article history:

Received: 30.08.2022

Accepted: 30.12.2022

Abstract: Even though the performance of photovoltaic/thermal (PV/T) panels had been examined both computationally and experimentally for some time, the thermal models created in earlier research were mostly steady-state models for estimating the annual yields. In this study, the solar thermal collector and photovoltaic (PV) cells are combined to create the PV/T collector, and water-ethylene glycol is utilized as a coolant to lower the temperature of the PV panels. The goal of this study is to analyze a water-ethylene glycol-based PV/T collector numerically. Time-dependent dynamic analyzes were performed using the MATLAB software program. Investigations were also done into how the electrical power produced and the temperatures of the fluid outlet and PV/T surface changed over time. As a result of the annual analysis, the maximum power of PV/T is calculated as 155 W. Also, the maximum surface temperature of PV/T panel's is 56.62°C.

Atıf için/To Cite:

Soytürk G. Kızıllkan Ö. Ezan MA. Mathematical modeling of a photovoltaic/thermal (PV/T) Collector. Uluslararası Teknolojik Bilimler Dergisi, 14(3), 144-152, 2022.

Bir fotovoltaiik termal (PV/T) kollektörün matematiksel modellemesi

Anahtar Kelimeler

Güneş enerjisi
Fotovoltaiik termal kollektör
Termal performans
Elektriksel performans

Makale geçmişi:

Geliş Tarihi: 30.08.2022

Kabul Tarihi: 30.12.2022

Öz: Fotovoltaiik-termal (PV/T) kollektörlerin performansı bir süredir hem hesaplamalı hem de deneysel olarak araştırılmış olsa da, daha önceki araştırmalarda oluşturulan termal modeller çoğunlukla yıllık verimleri tahmin etmek için kararlı hal modelleriydi. Bu çalışmada fotovoltaiik (PV) hücreler ve termal toplayıcı, PV/T toplayıcıyı oluşturmak için bir sisteme entegre edilmiştir ve su-etilen glikol, PV hücrelerinin sıcaklığını düşürmek için bir soğutucu olarak kullanılmıştır. Bu çalışmanın amacı, su-etilen glikol bazlı bir PV/T toplayıcıyı sayısal olarak analiz etmektir. Zamana bağlı dinamik analizler MATLAB yazılım programı kullanılarak yapılmıştır. Ayrıca PV/T yüzey sıcaklığının, akışkan çıkış sıcaklığının ve elde edilen elektriksel gücün zamanla değişimleri incelenmiştir.

1. Introduction

Renewable, also known as alternative energy resources, are resources that are inexhaustible and have the potential to be renewed. Since renewable energy resources are clean and environmentally friendly, energy production from these sources is increasing rapidly in our country and in the world. In addition to widely used energy sources like wind and solar energy, there are renewable energy resources such as hydrogen, biomass, and hydroelectricity used in different applications. Solar energy, which is widely used among renewable energy sources, has gained importance in

recent years to meet increasing energy needs. Solar energy is an inexhaustible, clean, environmentally friendly, free energy source that does not emit sulfur, carbon, and gas. The sun is the main energy source for all fuels used on earth, except nuclear fuels. Reactions occur in which hydrogen gas is constantly transformed into helium, the resulting mass difference is transformed into thermal energy and spreads, and a small part of this energy reaches the earth. Since gases such as carbon dioxide, ozone, and water vapor in the atmosphere absorb solar radiation, the sunlight reaching the earth is at low values. As can be seen in Fig. 1, our country has a very rich solar energy potential.

*Corresponding author: gamzeyildirim@isparta.edu.tr

New technologies are developing to evaluate this energy, and studies in this field are increasing day by day.

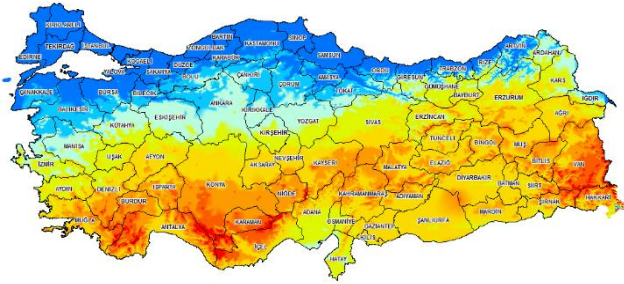


Figure 1. Sunbathing map of Türkiye [1]

Solar energy is mainly used for two different purposes: thermal energy and electrical energy. While various technologies are used for these aims, the efficiency of these technologies is increasing daily. Solar energy conversion to thermal energy takes place with solar collectors [2]. Photovoltaic technologies are widely used to obtain direct electrical power from solar energy [3].

Only 15% to 20% of solar energy can be converted into electricity when PV systems are utilized to generate electricity from it; the remainder is converted to thermal energy. This thermal energy can be easily absorbed by the PV device and causes the operating temperature to rise to 80°C [4]. The temperature of the PV solar panel reduces by about 0.2 – 0.5% for each degree Celsius as the solar radiation increases [5]. Large-scale heat extraction using a fluid circulation system that is induced or natural could solve this issue.

By simultaneously producing thermal and electrical energy, PV/T energy systems that feature combined PV cells and heat evacuation devices have developed an effective replacement for PV systems [6]. The PV/T systems seen in Figure 2, which are the result of innovative technologies in solar energy systems, allow the production of thermal and electrical energy at low temperatures by combining thermal collectors and photovoltaic cells. In these systems, PV cells in contact with the absorber surface co-convert some solar irradiation into electrical power, and the surplus heat energy produced in the PV cells is taken as the input of the thermal system. A heat carrier takes this heat from the surface and absorber cells when the system is in use. Thus, both the cells are cooled, thermal energy is obtained, and the panel's efficiency is increased [7]. PV/T panels could be categorized according to the various types of coolant used: water, air, and refrigerant. In addition, according to the physical design of the panels, they could be distinguished as concentrated, building integrated type, or flat plate type [8].

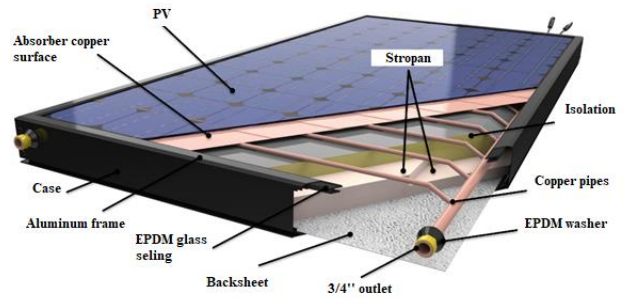


Figure 2. PV/T collector system elements [9]

Recently, study on PV/T systems has been increasing rapidly. Wolf [10], one of the first research articles on PV/T panels, evaluated the performances of a system in this study. His results showed that solar cogeneration systems are practically applicable. Rejeb et al. [11] focused on developing a PV/T and applied their designed model to optimize the operation of the PV/T panel in a semi-arid climate. Based on the energy balance of the collector's six major parts— PV cells, transparent cover, plate absorber, pipe, water in the pipe, and insulation—a model was created to predict the dynamic behavior of the collector. By comparing the experimental results that are available in the literature, they were able to demonstrate that there is a good agreement with the simulation results that were achieved. The electrical and heat energy of the tube collector and sheet were examined using the constructed model for four typical yearly days using the meteorological data for Tunisia. The effects of inlet water temperature, the number of glass covers, solar irradiation, and the conductive heat transfer coefficient between plate absorber and PV cells on thermal and electrical efficiency were also investigated using parametric analyses. A model for the simulation of a photovoltaic thermal collector in a transient regime was created and validated by Simonetti et al. [12]. On two hybrid PV/T solar tiles connected in series, they ran a two-week test in actual ambient weather conditions to validate the model. The average electrical efficiency was calculated by Joy et al. [13] to be 9.56% without cooling and 10.69% and 11.23% with water and water-ethylene glycol cooling, respectively. They carried out an experimental investigation of a PV panel using a mixture of water and water-ethylene glycol as the coolant. They also came to the conclusion that using water or water-ethylene glycol, respectively, resulted in the average thermal efficiency of the panel of 46.18% and 17.94%. Using nanofluids, Jia et al. [14] looked into the examination of a PV/T panel. Mathematical models of the PV/T panels were suggested in order to draw additional conclusions regarding how operating parameters affect the performance of the collector. They looked at the impact of nanofluid type and volume concentration on PV conversion efficiency, PV cell temperature, and thermal and electrical power in their

study. The results of a study on the effects of PV collector characteristics on performance were also discussed. They came to the conclusion that TiO_2 /water nanofluid performed worse in the PV/T collector than Al_2O_3 /water nanofluid did.

There are two various analyzes of PVT modeling in the literature. Firstly, it is based on numerical analysis by separately writing differential equations for all layers of the PV/T system. The second approach for the PV/T is making analyzes based on a single differential equation by considering it as a single layer. In this work, PV/T is considered as a single layer, and dynamic modeling is performed, in which both the PV/T surface temperature and the temperature changes of the heat transfer fluid over time.

2. Mathematical Modeling

In photovoltaic thermal systems, some solar irradiation is transformed into electrical energy, while a large part of it creates a thermal load on the material. This thermal load can reduce the collector's efficiency and damage the material's structure. PV/T systems have been designed to minimize this thermal load created by solar irradiation that cannot be converted into electrical energy in the collector. These hybrid systems can simultaneously provide hot air or domestic water and electrical power. The most widely used PV/T type is the system where hot water is provided. While these systems generate electrical energy with the modules on their upper surfaces, they store the domestic water with the copper plates on the back of the collector. Thanks to the working fluid in the collector, the temperature of the cell is diminished, and the electrical energy efficiency is raised [15]. The schematic representation of the PV/T panel is shown in Figure 3. As seen from the figure, the PV/T collector comprises a set of PV panel, a glass cover, pipes, an absorber surface, and insulation [13]. In Figure 3, the thermal resistance network of the PV/T panel is shown.

The following assumptions were considered in the PV/T mathematical modeling [16]:

- 1) PV/T panels are connected in series.
- 2) Air gaps between the glass cover and the PV cells are neglected.
- 3) PV/T is considered as a single layer, and heat transfer between layers is neglected.
- 4) PV/T mass and specific heat capacity are neglected.
- 5) Heat transfer by natural convection is neglected, and heat losses by wind are only considered for the upper surface of the collector.
- 6) The heat losses from the edge surfaces of the the PV/T panel are neglected.

- 7) The thermal capacities of the PV/T components are neglected. Only the thermal capacities of the heat transfer fluid are considered.

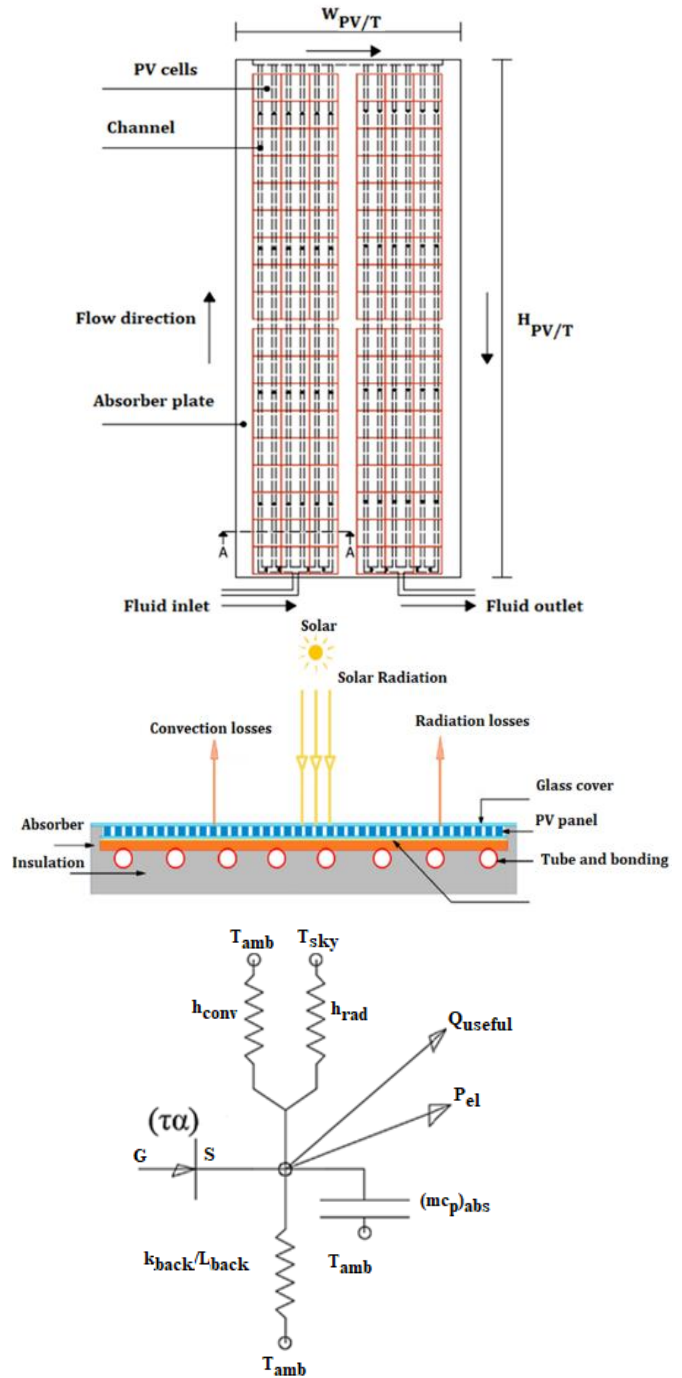


Figure 3. PV/T collector schematic and thermal resistance network (adapted from Ref. [15])

The properties of PV/T panel used in the mathematical modeling are given in Table 1.

Table 1. Properties of PV/T panel working with ethylene glycol –water mixture

Basic data		Value
PV/T length	L(m)	1.649 [9]
PV/T width	W (m)	0.992 [9]
PV/T total area	$A_{PV/T}$ (m ²)	1.635
PV/T cell area	A_{cell} (m ²)	1.417
PV/T mass	$m_{PV/T}$ (kg)	3.75
PV/T specific heat	$C_{pPV/T}$ (J/kgK)	8081
PV/T conductivity	$k_{PV/T}$ (W/mK)	187.1
PV/T thickness	$\lambda_{PV/T}$ (m)	0.0065
Absorptivity coefficient	α	0.85
Emissivity coefficient	ϵ	0.88
Transmissivity coefficient	τ	0.9
Packing factor	PF	0.9
Electrical data		
Cell type		p-Si
Reference efficiency	electrical η_{ref} (%)	0.143
Temperature coefficient	power β (1/K)	0.0046
Thermal data		
Mass flow rate	\dot{m}_{HTF} (kg/s)	0.002
Number of tube	n_{tube}	10
External tube diameter	D (m)	0.008
Internal tube diameter	D_i (m)	0.006
Distance between tubes	w (m)	0.099
Insulation thickness	λ_{back} (m)	0.03
Insulation conductivity	k_{back} (W/mK)	0.04
Boundary conductivity	k_{bond} (W/mK)	250
Boundary width	b_{bond} (m)	0.01
Boundary thickness	λ_{bond} (m)	0.05
Boundary heat transfer coefficient	h_{ca} (W/m ² K)	30.3214

In this work, heat that had accumulated in various parts of the hybrid solar system was removed using ethylene glycol-water as a heat transfer fluid. 50% by weight ethylene glycol-water mixture has been shown to have a higher energy and exergy efficiency than pure ethylene glycol and a lower freezing point than pure ethylene glycol when used as the working fluid for PV/T. As a result, ethylene glycol-water mixture (50 percent by weight) was utilized as a working fluid that was appropriate for cold climates. Temperature-dependent thermophysical properties for ethylene glycol (50%) were formulated using curve-fit curves from the Engineering Equation Solver (EES) [17] database. Required property values in the following equation:

$$y = a + bT + cT^2 + dT^3 + eT^4 + fT^5 + gT^6 \quad (1)$$

In the above equation, y is the thermophysical property (Cp, k, ρ, μ, Pr), and the coefficients a, b, c, d, e, f, and g are obtained for the temperature of T = 25°C and

pressure of P = 101.325 kPa. Various thermophysical property coefficients can be defined for different temperature and pressure values. These coefficients are obtained from the real table value with the help of curve-fitting methods. In determining the size of the linear regression error in curve fittings, the correlation coefficient 'R²' is determined. An R² value close to 1 means that the fitted curve best expresses the data. Table 2 shows the equation coefficients of the thermophysical properties of the water-ethylene glycol mixture (50% by weight).

Table 2. Coefficients of the thermophysical properties in Equation (1)

	Cp (kJ/kgK)	k (W/m ² K)	ρ (m ³ /kg)	μ (kg/ms)	Pr
a	3202.88	0.37	1074.62	0	67.19
b	5.64	0.0006	-0.43	-0.0002	-2.48
c	-0.008	3.17×10^{-7}	-0.002	0.000009	0.081
d	-0.0003	-50	0.000006	-42	-0.0029
e	0	0	0	7.3×10^{-9}	0.00006
f	0	0	0	-80.3	-64.7
g	0	0	0	2.39×10^{-13}	1.98×10^{-9}

The heat transfer coefficient of the working fluid in the pipe by convection is calculated as follows:

$$h_f = \frac{Nuk}{D_i} \quad (2)$$

Here, h_f (W/m²K) is the heat transfer coefficient of the fluid, and k (W/mK) is the thermal conductivity of the fluid. To calculate the h_f value of the working fluid, the Reynolds (Re) number must first be determined.

$$Re = \frac{\rho V D_i}{\mu} \quad (3)$$

where ρ (kg/m³) is the density of the fluid, V (m/s) is the velocity of the fluid, D_i (m) is the inner diameter of the pipe, and μ (kg/ms) is the absolute viscosity. If Re < 2500, laminar flow occurs, if Re ≥ 2500, turbulent flow occurs in the pipe [18].

L (m), the hydrodynamic inlet length, is expressed as the length from the pipe inlet where the shear stress (and, therefore, the friction factor) approaches the fully developed value by 2% [18]. The hydrodynamic inlet lengths in laminar and turbulent flow are calculated as follows:

$$L_{laminar} = 0.05ReD \quad (4)$$

$$L_{turbulent} = 10D \quad (5)$$

$$x^* = \frac{L}{RePrD} \quad (6)$$

Here, Pr is the Prandtl number, and D (m) is the hydraulic diameter.

The Nusselt number for thermally developing laminar flow is determined by Equation (7) and Equation (8):

$$Nu = 1.953(x^*)^{-\frac{1}{3}} \quad x^* \leq 0.03 \quad (7)$$

$$Nu = 4.364 + \frac{0.0722}{(x^*)^{-\frac{1}{3}}} \quad x^* > 0.03 \quad (8)$$

In the case of turbulent flow, the Nusselt number can be determined by Equation (9) as [18]:

$$Nu = \frac{\frac{f}{8}(Re - 1000)Pr}{1 + 12.7\left(\frac{f}{8}\right)^{\frac{1}{2}}\left(\frac{2}{3}Pr - 1\right)} \quad (9)$$

Here f is the friction factor, and it is determined by Equation (10) [15]:

$$f = \frac{1}{(0.79 \ln(Re) - 1.64)^2} \quad (10)$$

The total heat loss coefficient U_L (W/m²K) in the collectors is calculated by Equation (11). Here, U_e (W/m²K) heat losses from the side surfaces are disregarded, while the total heat loss from the collector is calculated with the sum of the heat losses from the upper and lower surfaces [18]:

$$U_L = U_t + U_b \quad (11)$$

where U_t (W/m²K) denotes the heat loss coefficient from the collector top surface, and U_b (W/m²K) represents the loss coefficient from the collector back surface [15]:

$$U_t = h_{conv} + h_{rad} \quad (12)$$

Here, h_{conv} (W/m²K) denotes the heat transfer coefficient with forced convection, and h_{rad} (W/m²K) denotes the heat transfer coefficient with radiation [15]:

$$h_{conv} = 2.2V_{wind} + 8.3 \quad (13)$$

$$h_{rad} = \varepsilon\sigma(T_{PV/T}^2 + T_{sky}^2)(T_{PV/T} + T_{sky}) \quad (14)$$

$$T_{sky} = 0.0552T_{amb}^{1.5} \quad (15)$$

Here, V_{wind} (m/s) represents the average wind speed, $T_{PV/T}$ (K) means the average PV /T surface temperature, T_{sky} (K) represents the sky temperature, and T_{amb} (K) the ambient temperature [19]:

$$U_b = \frac{k_{back}}{\lambda_{back}} \quad (16)$$

Here, k_{back} (W/mK) represents the thermal conductivity of the back surface insulation material, and λ_{back} (m) refers to the thickness of the back surface insulation material.

A one-dimensional steady-state model was developed to study the thermal and electrical efficiency of PV/T systems, and Hottel-Whillier equations were employed in these calculations. The overall energy balance of the PV/T collector is calculated by Equation (17) [16]:

$$\dot{Q}_u = F_R \left(I(\alpha\tau)(A_{PV/T} - A_{cell}\eta_{el}) - (A_{PV/T}U_L(T_{in} - T_{out})) \right) \quad (17)$$

Here, \dot{Q}_u (W) represents the useful heat supplied from the collector, I (W/m²) solar radiation, $(\alpha\tau)$ absorbance-permeability coefficient, η_{el} collector electrical efficiency, $A_{PV/T}$ (m²) collector surface area, A_{cell} (m²) PV/T cell area, T_{in} (K) fluid inlet temperature.

The collector heat gains factor (F_R) is calculated by Equation (18) as follows [19]:

$$F_R = \frac{\dot{m}_{HTF}c_p}{A_{PV/T}U_L} \left(1 - \exp\left(\frac{-A_{PV/T}U_L F'}{\dot{m}_{HTF}c_p}\right) \right) \quad (18)$$

Here, \dot{m}_{HTF} (kg/s) is the mass flow rate of the fluid, c_p (J/kgK) is the specific heat capacity of the fluid, and F' is the collector efficiency factor.

$$F' = \frac{\frac{1}{U_L}}{w \left(\frac{1}{U_L(D + (W - D)F)} + \frac{1}{h_{ca}} + \frac{1}{\pi D_i h_f} \right)} \quad (19)$$

Here, w (m) is the space between the pipes through which the PV/T fluid passes, D (m) is the outer diameter of the tube, h_{ca} (W/m²K) is the boundary heat transfer coefficient, D_i (m) is the inner diameter of the tube, h_f (W/m²K) represents the heat transfer coefficient of the fluid.

$$F = \frac{\tanh\left(\frac{m(w - D)}{2}\right)}{\frac{m(w - D)}{2}} \quad (20)$$

The value of m here is calculated by Equation (21):

$$m = \sqrt{\frac{U_L}{(k\lambda)_{PV/T}}} \quad (21)$$

P_{el} , which is the electrical power gained from PV/T, is calculated by Equation (22) [16]:

$$P_{el} = \eta_{el} I A_{cell} (\alpha \tau) \quad (22)$$

Average PV/T temperature $T_{PV/T}$ is calculated by Equation (23) [15]:

$$T_{PV/T} = T_{in} + \left(\frac{\dot{Q}_u}{A_{PV/T} F_R U_L} \right) (1 - F_R) \quad (23)$$

Also, the fluid mean outlet temperature T_{HTF} (K) can be found by Equation (24):

$$T_{HTF} = \dot{Q}_u + \frac{\dot{m}_{HTF} c_p (T_{in} - T_{out})}{m_{HTF} c_p} + T_{out} \quad (24)$$

Electrical and thermal efficiencies of PV/T could be calculated using Equation (25) and Equation (26) [20]:

$$\eta_{el} = \eta_{ref} \left(1 - \beta \left(T_{PV} - T_{amb} \right) \right) \quad (25)$$

Here, η_{ref} denotes the electrical efficiency at the reference point, and β denotes the temperature power coefficient.

$$\eta_{th} = \frac{\dot{m}_{HTF} c_p (T_{HTF} - T_{in})}{I (\alpha \tau) A_{PV/T}} \quad (26)$$

The total efficiency of the PV/T system is determined by Equation (27):

$$\eta_{PV/T} = \eta_{el} + \eta_{th} \quad (27)$$

3. Results and Discussion

This study develops and validates a model for the simulation of a hybrid PV/T panel in the transient regime. Generally speaking, the model was created using MATLAB simulation software. For the time-dependent dynamic models to be made in this study, it is necessary to determine the annual solar radiation, environmental temperature, and wind speed changes of İzmir province. For this purpose, yearly meteorological data of İzmir province were taken from the Meteonorm [21] library in TRNSYS software and shown in Figure 4.

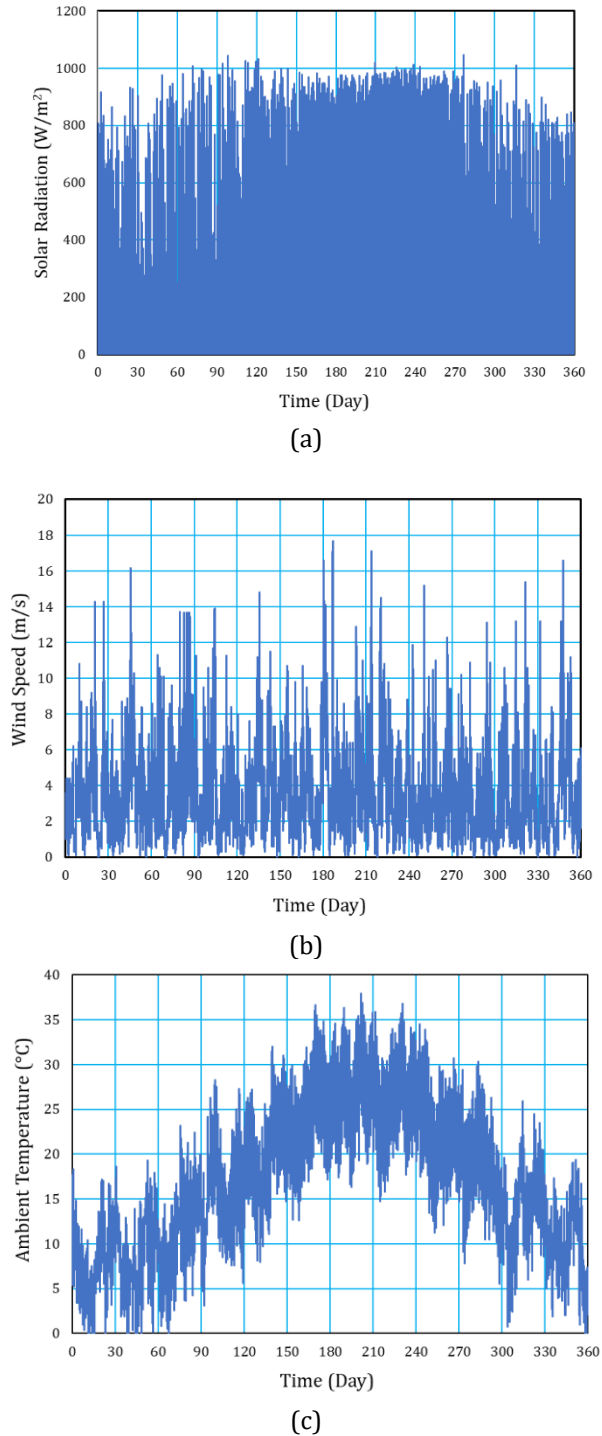


Figure 4. Annual meteorological data for İzmir (a) Solar irradiation intensity (b) Wind speed (c) Ambient temperature

In Figure 5, the graph of variation of the collector flow factor (F'') and the dimensionless number $(\dot{m} c_p) / (A U_L F')$ in the reference study by Duffie and Beckman [22] was shown to validate the current mathematical model. As can be seen from the figure, the trend in the PV/T mathematical modeling and the trend in the reference study are compatible with each other.

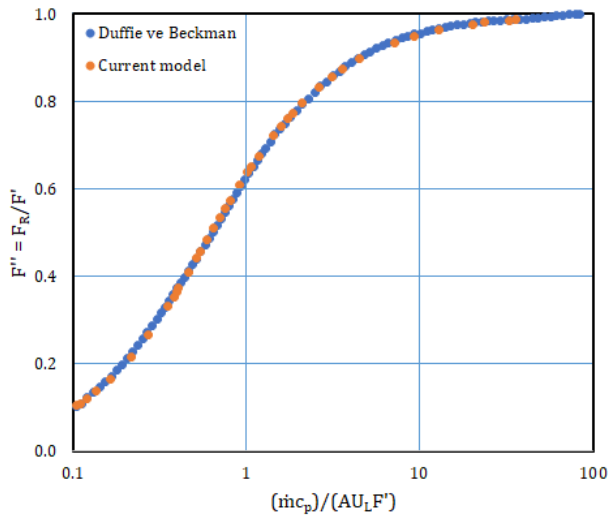


Figure 5. PV/T collector flow factor F'' as a function of $(\dot{m}_{HTF} C_p)/(A_{PV/T} U_L F')$

Figure 6 depicts the PV/T surface temperature's fluctuation over the first three days of January. The PV/T surface temperature rises as solar irradiation rises, as shown in the figure. The three-day analysis produced a maximum panel temperature estimate of about 40°C.

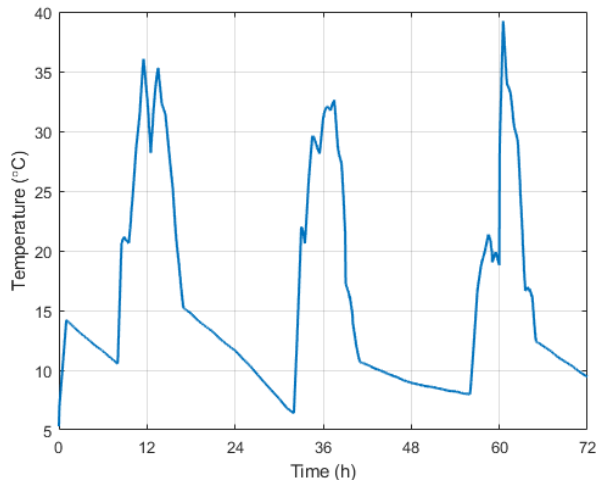


Figure 6. Variation of the PV/T surface temperature with time

Figure 7 shows the change in the heat transfer fluid's output temperature over time. The output temperature of the heat transfer fluid rises with an increase in solar radiation, as seen in the image. The maximum exit temperature of the heat transfer fluid was determined

to be almost 14°C as a result of the three-day analysis.

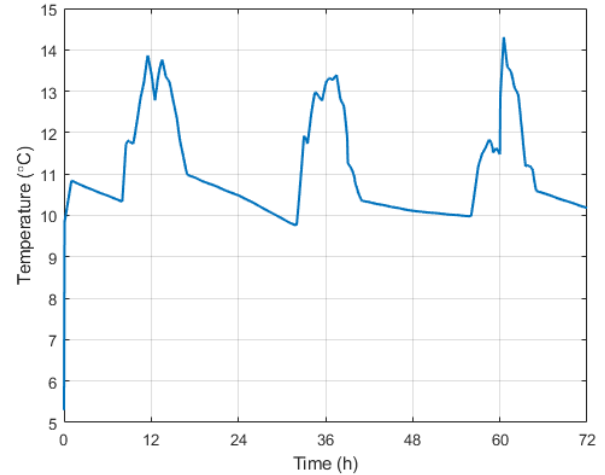


Figure 7. Variation of the outlet temperature of the heat transfer fluid with time

The electrical power's change over time is depicted in Figure 8. Throughout the analysis time, the solar radiation value changed simultaneously with the electrical power produced by the PV collector and the PV/T panel, and the highest electrical efficiency was attained at noon when the radiation was at its highest.

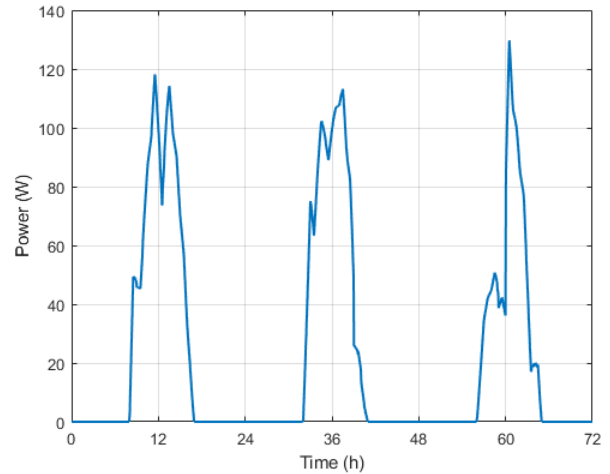


Figure 8. Variation of the electrical power with time

Figure 9 depicts the fluctuation in the working fluid outlet temperature and PV/T surface temperature for the chosen three days. The change of the PV/T surface temperature and the working fluid outlet temperature follow the same trend, as shown in the figure. In rare circumstances, the working fluid's output temperature climbs above the PV/T surface temperature. This is due to the fact that just the mass and specific heat of the working fluid are taken into account in the PV/T mathematical modeling, but the PV/T has no resistance and heats up and cools down quickly.

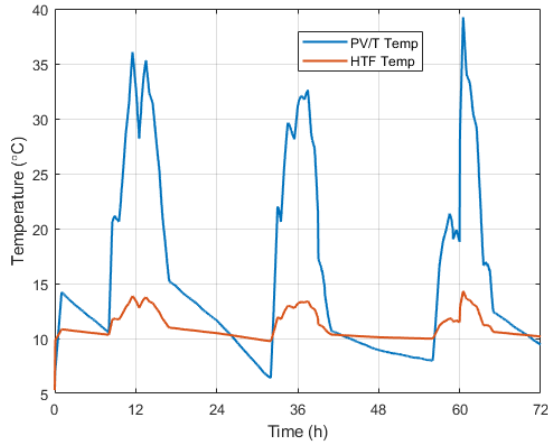


Figure 9. Variation of the outlet temperature of the heat transfer fluid and PV/T surface temperature with time

Figure 10 shows the thermal efficiency based on the $(T_{in} - T_{amb}) / I_{solar}$ ratio, which is an indicator for evaluating the performance of PV/T. As can be observed in the figure, for flow rates of 0.03, 0.1, 0.2, 0.3, and 0.36 kg/s, there was a tendency for thermal efficiency to decrease as the $(T_{in} - T_{amb}) / I_{solar}$ increased due to the rise in heat losses due to the temperature difference between the working fluid and the ambient air. In addition, verification studies were carried out considering the reference study of Kim and Kim [23], and the average efficiency at a flow rate of 0.36 kg/s reached the highest value of 40% when the difference between the inlet temperature and the ambient temperature was zero. As seen in the figure, in the current study, thermal efficiency reaches 40% from 26% by raising the mass flow rate from 0.03 kg/s to 0.36 kg/s under 800 W/m² radiation conditions.

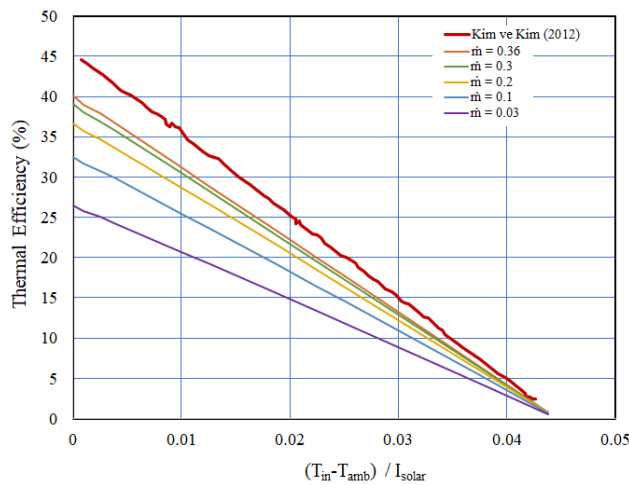


Figure 10. PV/T thermal efficiency curve according to $\Delta T / I_{solar}$

The variation of the electrical efficiency of PV/T according to the temperature difference is shown in

Figure 11. As in thermal efficiency verification studies, electrical efficiency variation was observed for flow rates of 0.03, 0.1, 0.2, 0.3, and 0.36 kg/s depending on the $(T_{in} - T_{amb}) / I_{solar}$ ratio. As can be seen in the figure, verification studies were carried out with the reference study of Kim and Kim [23], and it was observed that the $\Delta T / I_{solar}$ ratio and the electrical efficiency tended to decrease.

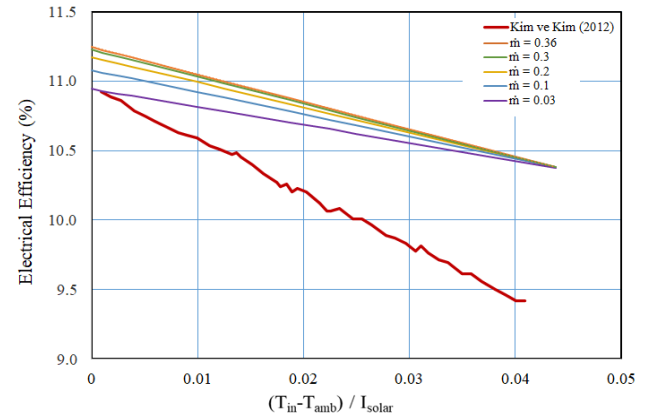


Figure 11. PV/T electrical efficiency curve according to $\Delta T / I_{solar}$

4. Conclusions

In this study, a mathematical model was conducted with the purpose of validating the water-ethylene glycol-based PV/T panel. Based on the energy balance of the PV/T panel, which is made up of several parts, including PV cells, insulation, transparent cover, pipes, plate absorber, and fluid inside the pipe, a model has been created to predict the dynamic behavior of the PV/T panel. Comparing the data found in the literature allowed us to confirm that the obtained theoretical results were in good agreement. During the analyses, the mass flow rate was taken as 0.02 kg/s, and the change of PV/T surface temperature, fluid outlet temperature, and electrical power over time was calculated for three days selected in İzmir conditions. As a result of analysis, the maximum surface temperature of PV/T panel's is 56.62°C. Also, the maximum power of PV/T is calculated as 155 W.

Acknowledgment

This research was supported by The Scientific and Technological Research Council of Turkey (TUBITAK) with project number 220N405.

References

- [1] GEPA (Güneş Enerjisi Potansiyeli Atlası) <https://gepa.enerji.gov.tr/MyCalculator/> (Date of Access: 26.08.2022).
- [2] Soytürk Yıldırım G. Investigation of the use of solar energy in the storage and heating applications with phase changing material. MSc Thesis, Süleyman Demirel University, Isparta, Turkey, 2018 (In Turkish).
- [3] Kazemian A, Taheri A, Sardarabadi S, Ma T, Fard MP, Peng J. Energy, Exergy and Environmental Analysis of Glazed and Unglazed PVT System Integrated with Phase Change Material: An Experimental Approach. *Solar Energy*, 201, 178-189, 2020.
- [4] Ma T, Yang H, Zhang Y, Lu L, Wang X. Using Phase Change Materials in Photovoltaic Systems for Thermal Regulation and Electrical Efficiency Improvement: A Review and Outlook. *Renewable and Sustainable Energy Reviews*, 43, 1273-1284, 2015
- [5] Babayan M, Mazraeh AE, Yari M, Niazi NA, Saha SC. Hydrogen Production with a Photovoltaic Thermal System Enhanced by Phase Change Materials, Shiraz, Iran Case Study. *Journal of Cleaner Production*, 215, 1262-1278, 2015
- [6] Gül M, Akyüz E. Hydrogen Generation from a Small-Scale Solar Photovoltaic Thermal (PV/T) Electrolyzer System: Numerical Model and Experimental Verification, *Energies*, 13, 2997, 2020.
- [7] Sachit FA, Rosli MAM, Tamaldin N, Misha S, Abdullah AL. Nanofluids Used in Photovoltaic Thermal (PV/T) Systems: A Review. *International Journal of Engineering & Technology*, 7, 599-611, 2018.
- [8] Zulkepli A, Ibrahim H, Alias A, Azran Z, Basrawi F. Review on the recent developments of photovoltaic thermal (PV/T) and proton exchange membrane fuel cell (PEMFC) based hybrid system. *MATEC Web of Conferences*, 2016.
- [9] Solimpeks. <https://www.solimpeks.com.tr/> (Date of Access: 25.03.2022)
- [10] Wolf M. Performance Analyses of Combined Heating and Photovoltaic Power Systems for Residences, *Energy Conversion*, 16 (1), 79-90, 1976.
- [11] Rejeb Q, Dhaou H, Jemni A. A Numerical Investigation of a Photovoltaic Thermal (PV/T) Collector. *Renewable Energy*, 77, 43-50, 2015
- [12] Simonetti R, Molinaroli L, Manzolini G. Development and Validation of a Comprehensive Dynamic Mathematical Model for Hybrid PV/T Solar Collectors. *Applied Thermal Engineering*, 133, 543-554, 2018.
- [13] Joy B, Zachariah R. Experimental Investigation and Comparative Study of PV Thermal Water- Ethylene Glycol Collector and PV System. *International Journal of Current Engineering and Scientific Research (IJCESR)*, 2(9) ,2394-0697, 2015.
- [14] Jia Y, Ran F, Zhu C, Fang G. Numerical Analysis of Photovoltaic-Thermal Collector Using Nanofluid as a Coolant. *Solar Energy*, 196, 625-636, 2020.
- [15] Benli F. Experimental comparison of photovoltaic (PV) and photovoltaic-thermal (PV-T) collectors. MSc Thesis, Osmaniye Korkut University, 2018 (In Turkish).
- [16] Sakellariou E, Axaopoulos P. An Experimentally Validated, Transient Model for Sheet and Tube PVT Collector. *Solar Energy*, 174, 709-718, 2018.
- [17] Engineering Equation Solver (EES). <https://fchartsoftware.com/ees/> (Date of Access: 25.03.2022)
- [18] Çengel YA, Ghajar A. Heat and Mass Transfer, McGraw Hill Education, 5e, 2014.
- [19] Kalogirou SA. Solar Energy Engineering Processes and System, Elsevier, 2015.
- [20] Yazdanifard F, Ebrahimnia-Bajestan E, Ameri Mehran. Investigating the Performance of a Water-Based Photovoltaic/Thermal (PV/T) Collector in Laminar and Turbulent Flow Regime. *Renewable Energy*, 99, 295-306, 2016.
- [21] Energy Economics, Energy Charting Tool. <https://www.bp.com/en/global/corporate/energy/economics/energy-charting-tooldesktop.html> (Date of Access: 20.03.2022).
- [22] Duffie JA, Beckman WA. Solar Engineering of Thermal Processes (4th ed.). New York: Wiley, 2013.
- [23] Kim JH, Kim JT. Comparison of Electrical and Thermal Performances of Glazed and Unglazed PVT Collectors. *International Journal of Photoenergy*, 2012.